AD-A131 018 METALLURGICAL CHARACTERIZATION OF NIOBIUM/TIN SUPERCONDUCTING MULTIFILAME..(U) RICE UNIV HOUSTON TX DEPT OF MECHANICAL ENGINEERING J M ROBERTS 31 MAR 83 AFOSR-TR-83-0596 AFOSR-82-0150 F/G 11/6 NL

1/1

UNCLASSIFIED

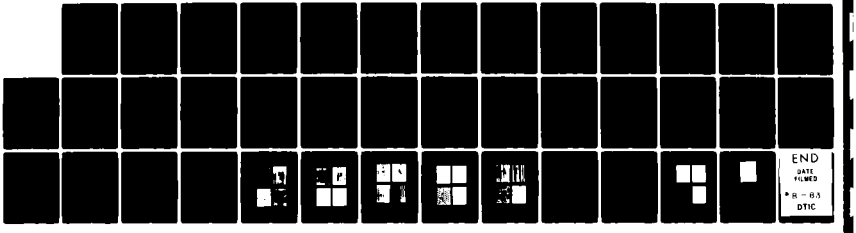

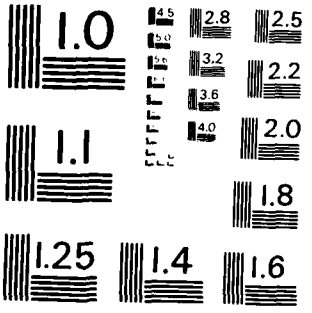

UNCLASSIFIED

SECURITY CLASSIFICATION OF THIS PAGE (When Data Entered)

REPORT DOCUMENTATION PAGE

READ INSTRUCTIONS BEFORE COMPLETING FORM

1. REPORT NUMBER: AFOSR-TR- 83-0596	2. GOVT ACCESSION NO.: AD-A131018
3. RECIPIENT'S CATALOG NUMBER:	
4. TITLE (and Subtitle): Metallurgical Characterization of Niobium/Tin Superconducting Multifilamentary Wires	5. TYPE OF REPORT & PERIOD COVERED: Final Report April, 1982-December, 1982
	6. PERFORMING ORG. REPORT NUMBER:
AUTHOR(s): Dr. John Melville Roberts	8. CONTRACT OR GRANT NUMBER(s): AFOSR-82-0150
PERFORMING ORGANIZATION NAME AND ADDRESS: Rice University, P. O. Box 1892, Houston, Texas 77251	10. PROGRAM ELEMENT, PROJECT, TASK AREA & WORK UNIT NUMBERS: 61102F 2306/D9
CONTROLLING OFFICE NAME AND ADDRESS: United States Air Force, Air Force Office of Scientific Research, Building 410, Bolling AFB, D.C. 20332	12. REPORT DATE: 1983 March 31
	13. NUMBER OF PAGES: 27 pages plus 9 pages of figures
MONITORING AGENCY NAME & ADDRESS(if different from Controlling Office)	15. SECURITY CLASS. (of this report): Unclassified
	15a. DECLASSIFICATION DOWNGRADING SCHEDULE

16. DISTRIBUTION STATEMENT (of this Report)

Approved for public release; distribution unlimited.

17. DISTRIBUTION STATEMENT (of the abstract entered in Block 20, if different from Report)

18. SUPPLEMENTARY NOTES

19. KEY WORDS (Continue on reverse side if necessary and identify by block number)

Superconductor, Fine Filament, Niobium/Bronze, Metallurgical Characterization

20. ABSTRACT (Continue on reverse side if necessary and identify by block number)

The origin of a high incidence of discontinuous Nb filaments in Niobium/bronze multifilamentary drawn wires is discussed. It is suggested their occurrence is most likely an intrinsic part of the manufacturing process. Studies on the application of the "limiting grain size" concept in the bronze by the Nb filaments, suggests this effect only sets an upper bound on the attainable grain size and in reality, the actually observed grain size and sub-grain size is lower (continued on back)

DD FORM 1 JAN 73 1473 EDITION OF 1 NOV 65 IS OBSOLETE

UNCLASSIFIED

SECURITY CLASSIFICATION OF THIS PAGE (When Data Entered)

20. Abstract (continued)

than this upper bound. This leads to extensive hardening of the bronze phase as the Nb/bronze multifilamentary wires are progressively reduced to ultra-fine dimensions. Preliminary ageing studies of a 13 wt % Sn bronze alloy, suggest the α bronze may exhibit some age hardening decomposition phenomena in the 300 to 400°C temperature range for unprestrained solution heat treated and quenched material. An even stronger hardening phenomena in this temperature range occurs if the material is prestrained 65% in compression after solution heat treatment but prior to ageing. Contemplated further studies in the area are presented.

FINAL SCIENTIFIC REPORT SUBMITTED TO THE AIR FORCE OFFICE OF SCIENTIFIC RESEARCH AS MINI-GRANT No. 82-0150 EXTENSION TO THE SUMMER FACULTY RESEARCH PROGRAM ADMINISTERED FOR AFOSR UNDER CONTRACT WITH THE SOUTHEASTERN CENTER FOR ENGINEERING EDUCATION ENTITLED:

METALLURGICAL CHARACTERIZATION OF NIOBIUM/TIN SUPERCONDUCTING MULTIFILAMENTARY WIRES

PRINCIPAL INVESTIGATOR: John Melville Roberts

INSTITUTION: William Marsh Rice University
Department of Mechanical Engineering
and Materials Science
P. O. Box 1892
Houston, Texas 77251

EFFECTIVE DATE: 1982, April 01 : Duration - 6 months

with an added 3 months - no new fund extension.

TERMINATION DATE: 1982, December 31.

REPORT DATE: 1983 March 31

ABSTRACT

Reasoning is presented to suggest a mechanism for the occurrence of discontinuous Nb oversized filaments in Nb/Bronze superconducting wires. It is suggested the Nb filaments neck down or fracture as a result of differential tensile stresses in the Nb and bronze phases and substantial interfacial shear stress between these phases being developed during both the wire drawing and anneal cycle operations. The origin of these stresses is related to the different yield stress of the Nb and the bronze during drawing and is related to the different thermal expansion coefficients of these phases during annealing. The high incidence of these discontinuous filaments is believed to contribute to the optimum potential electrical properties of these wires not being fully attained. Studies on the application of the "limiting grain size" concept in the bronze by the Nb filaments, suggests this effect only sets an upper bound on the attainable grain size and in reality, the actually observed grain size and sub-grain size is lower than this upper bound. This leads to extensive hardening of the bronze phase as the Nb/bronze multifilamentary wires are progressively reduced to ultra-fine dimensions. Preliminary ageing studies of a 13 wt% Sn bronze alloy, suggest the α bronze may exhibit some age hardening decomposition phenomena in the 300 to 400°C temperature range for unprestrained solution heat treated and quenched material. An even stronger hardening phenomena in this temperature range occurs if the material is prestrained 65% in compression after solution heat treatment but prior to ageing. Contemplated further studies in the area are presented.

I. INTRODUCTION

Objectives and Statement of Work

The manufacturing process used in producing Nb_3Sn composite wires in sufficiently long lengths to be useful in the winding of superconducting magnets or generators by the internal bronze process has been recently discussed by Royet[1]. Ho[2] et. al. had pointed out that control of the draw-anneal sequences and conductor geometry had not been evaluated sufficiently to ensure that Nb_3Sn multifilament conductor can be produced by the bronze process in a repeatable and reliable manner. Royet[1] concludes that the achievement of the finest wire and filament diameters was hampered by wire breakage during manufacture. Royet[1] found that extensive deformation (four 17% reduction in area draws) of a 13 wt. % Sn bronze alloy which had been homogenized at 700°C for 120 hours exhibited some apparent embrittlement ageing characteristics. That is, room temperature ageing for some 77 hours apparently made the material brittle with zero % reduction in area in a tensile test compared to 41% reduction in area just after processing. This was clearly not conclusive proof of any ageing process in the bronze at room temperature, however, since the brittle sample could have contained some inhomogenized tin rich second phase[3][4] or a large casting porosity region[4].

This marked change in the percent reduction in area could certainly be evidence of a true α bronze embrittlement phenomena at room temperature, possibly due to grain boundary and dislocation segregation effects raising the yield stress close to the ultimate tensile stress. Royet[1] did not report the yield stress behavior in this test, but the total elongation to failure for both samples was very low i.e. about 1.24% and 0.58% for the 41% and 0% reduction in area samples respectively.

These very low percent elongations to failure really suggest both types of samples, irrespective of ageing time at room temperautre i.e. 0 or 77 hours were essentially brittle with respect to longitudinal tensile strain properties.

Another ageing experiment performed by Royet[1] on the same 13 wt % tin bronze suggested a marked enhanced work-hardening behavior in 40% reduced bronze wires after 7 days of ageing at room temperature, yet no significant change occurred in the first 14 hours. Again, the current investigator feels that these limited tests cannot be considered as serious evidence for any real embrittlement effect of this 13 wt % Sn bronze at room temperature after extensive strain. Again, it may have just happened tha. the apparently brittle tensile sample contained some tin rich second phase or large casting porosity region.[3,4] However, grain boundary tin segregation after 7 days at room temperature is a possible explanation which cannot be ruled out completely.

The overall objectives of this research were to study the ageing characteristics of 13 wt % tin bronze, in particular to try and evaluate if any form of α phase decomposition with attendant property changes occurs as a result of zero or some prestrain in the temperature region, room temperature at 400°C. It was planned to study thin foil samples via transmission electron microscopy to look for evidence of any tin rich grain boundary precipitation or any form of tin rich decomposition product from the metastable α phase.

It was also an overall objective of the research to investigate what effect the "limiting bronze grain size effect" and associated "mean free bronze path" and "limiting sub-grain size" effect may have upon the overall quality limits of the current Nb_3Sn superconducting multifilamentary manufacturing wire process.

Attempts were to be made to try and evaluate the origin of oversized discontinuous Nb filaments which have been observed in these multifilamentary Niobiom/Bronze wires.

II. STATUS OF THE RESEARCH

II(A) Discontinuous Nb Filaments in the Multifilamentary Nb Wires

In approximately 4.5 inches of annealed IGC (Intermagnetics General Corporation) 0.0274 in. diameter multifilamentary bronze/Nb wire, the current investigator found 20 discontinuous filaments in one cross-section alone. In general, the defects occurred near the center of the wire. Since one cross-section views 108 to 130 Nb filaments and if we assume about the same density of discontinuous filaments occurs in other cross-sections, these preliminary results suggest that about 20 to 15% maximum of the Nb filaments are discontinuous in a 4.5 inch length of wire. This infers that almost all of the central Nb filaments have about one discontinuous defect every two feet of wire. In practically all cases, each discontinuous filament was associated with hair line cracks at one end of the filament and sometimes at both ends of the filament. Oftentimes, cracks flow from beside the discontinuous filament to its tip. Figs. 1 through 10 show typical examples of these discontinuous Nb filaments with their associated hair-line crack patterns. Fig. 11 shows a Nb filament which appears to have fractured, yet is not of the oversized type. These are all Scanning Electron Micrographs of the carefully mounted and polished specimens.

The origin of the hair line crack is of interest. In the wire drawing process, metal must flow normal to the die face and then subsequently in the drawing direction. It is further recalled, that the present investigator has never found any second phase or tin

enriched regions around a discontinuous Nb filament, only cracks or large void cavaties. From a study of these discontinuous Nb filaments, it appears the hair line cracks are a cause and not the effect of the discontinuous filament. The current investigator believes these discontinuous filaments which have not manifested themselves to the extent of wire breakage probably arise by two mechanisms.

The first mechanism would be at a bronze site which contained a porosity pit in the original casting. If this porosity pit has not fully cohered to the matrix in the extrusion process steps, then the flow of the bronze at the pit site during wire drawing is disturbed. In fact, the flow should be slowed down and this restricts or pinches off the softer Nb filaments, hence the latter ball out. Possible examples of this mechanism are shown in Figs. 6 through 10.

The second mechanism considers how the wire draw force is distributed across the composite cross-section of the wire. It is patently clear that the tensile draw stresses can not be equal in the bronze and Nb phases, even if the volume fraction of each phase is 0.5. This is because of the differences in flow stress, Young's modulus of elasticity and Poisson's ratio of the two materials i.e. Nb and 13 wt % Sn bronze, which are in intimate contact. As long as the tensile stress applied to the wire during drawing is less than the tensile yield stress of the materials being drawn, satisfactory wire drawing is possible[5]. It is possible that for about 10% reduction in area passes of the wire, the yield stress of the Nb filaments may be exceeded and hence they flow excessively or may even fracture, yet the surrounding bronze remains continuous. Subsequent flow of metal on each side of the broken wire can cause restriction to its elongation and it balls out. Typical examples of this type of possible failure mechanism are shown in Figs. 1-5 and 11. It is clear these differential tensile stress levels in the 2 phases will set-up strong interfacial shear stresses

as long as the interfaces remain intact[6]. Relaxation of these strong shear stresses could explain the sheared Mode II type of fracture lines discernible in Fig. 4 for example. However, it appears this mechanism causes dominantly a Mode I type of tensile fracture of the homogeneously or inhomogeneously strained Nb filament (see Figs. 1-3, 5 and 11).

This second proposed mechanism for the formation of the discontinuous Nb filaments with their attendant hair line cracks has a natural extension. The linear thermal expansion coefficients of Nb[7], Cu[7] and 8% Sn bronze[8] are 7.3×10^{-6}, 17.0×10^{-6} and 18×10^{-6} per °K respectively. Since, Nb has a linear thermal expansion coefficient less that 1/2 that of Cu or the bronze, rather large differential tensile and interfacial shear stresses will be set up between the Nb and the bronze during annealing cycles[6]. The current investigator thus concludes the discontinuous Nb filament fractures could be initiated either during the wire drawing operation and/or during the annealing cycle operation. The generally excellent fracture toughness properties of the α bronze prevents the fractures to lead to catastrophic failure in most cases upon subsequent anneal and wire drawing cycles. This is clearly a situation which becomes more severe as the bronze work hardens with continued drawing and annealing of the wires to finer and finer overall diameters.

We cannot rule out, however, that at each one of the cracks or cavaties near the discontinuous filament, a Sn rich precipitate phase existed as a hard spot to restrict metal flow. This would mean in all cases, this precipitate has been pulled out of the sample and lost in the polishing operations since we have never detected the existence of any tin rich regions near the discontinuous filaments. The current investigator considers this explanation highly unlikely. Only a small percentage of the

discontinuous Nb filaments probably form from this effect since the brittle Sn rich phase would most likely fracture early on in the drawing process and cause a full cross-section wire breakage.

The first proposed mechanism, i.e. unhealed porosity sites in the cast bronze causing discontinuous filament formation is not an intrinsic limitation upon the manufacturing process. This can be controlled as well as the existence of tin rich phases by thorough degassing, working and homogenization of the bronze. This investigator does not believe this is a dominant origin of the discontinuous filaments. The present investigator believes these filaments generally arise from differential tensile stresses in the Nb and bronze phases during drawing and thermal annealing, with the attendant fracturing of the Nb filaments or shear failures along the Nb/bronze interfaces. This mechanism places a basic manufacturing limitation upon this process, since this effect can only be somewhat reduced by making smaller and smaller percent reduction in area wire passes per anneal cycle to prevent catastrophic breakage during drawing. Annealing should probably be done in an enert atmosphere for the final draw passes in producing ultra fine multifilamentary wires to ensure the Nb will not pick-up any hydrogen. The wire should be cooled rapidly from the annealing temperature of about 450°C to 250°C and slowly cooled thereafter to ensure no possible embrittlement of the bronze. All of these remedies are certainly going to raise the cost of the wire fabrication.

If more and more Nb/bronze hair line cracks form during increased number of annealing cycles, as a result of the differential thermal expansions of Nb, Cu and α Sn bronze, then it appears there is only one possible way to circumvent the continued formation of these

defects. This solution would apply to the bronze process of making multifilamentary Nb_3Sn wires via either the internal or external bronze process. This solution is presented by Royet[1] wherein he states "We think the Nb_3Sn multifilamentary conductor can be manufactured if a continuous hot drawing method is developed and used after the last restack-extrusion step." The present investigator agrees that such a hot drawing operation will minimize if not eliminate the differential stress situation between the Nb and bronze phases which is currently being developed during the cyclic annealing stages.

There is, however, no assurance a continuous hot drawing process (depending upon the specific hot drawing temperature) may not lead to oxidation problems or some α bronze phase decomposition problems. In addition, it is most likely that continuous hot drawing would not eliminate the differential stress situation between the α bronze and Nb phases which occur during the drawing operation itself. Consequently, discontinuous Nb filaments may continue to form and possible mechanical breakage at these sites in the final wire drawing stages may prevail.

The existence of the apparently high density of these discontinuous Nb filaments, and which are expected to be discontinuous after the reaction to form Nb_3Sn filaments, should affect the electrical quality of the superconductor. In particular, this may be the reason the critical current densities in commercially bronze processed Nb_3Sn multifilamentary superconducting wires exhibit significantly different values depending upon the manufacturer and on the details of the heat-treatment and fabrication steps. The best critical current density values in multifilamentary wires are about a factor of two lower than the value measured in monofilamentary Nb_3Sn wires[9]. The development of a continuous hot drawing process may improve this situation, but this investigator is not optimistic such a process will eliminate the discontinuous Nb filament problem.

II(B) Limiting Bronze Grain Size Effect

Numerous anneal cycles are required in an attempt to soften the bronze after several wire reduction passes. It is well known that second-phase inclusions are known to put an upper limit on the grain size of a metal[10]. During annealing and recrystallization, the strain free grains migrate and move into the strained matrix. After recrystallization is complete, grain coarsening can occur to lower grain boundary surface energy. In both processes, the migrating boundaries are interrupted at the second phase filaments, and the boundaries form curvatures and try to pull-away from the second phase obstacles. Once the migrating grain boundary or low angle sub-grain boundary has trapped so many inclusions (Nb filaments here), that the surface tension force, which is small due to its lack of curvature, cannot overcome the restraining force of the inclusions, the grain size has been limited.

We consider the Nb rods as second phase particles limiting the bronze grain size upon recrystallization. Under these conditions it is easily shown:

$$R = \frac{2}{n_s \pi r} \qquad (1)$$

where R is the upper limit on the bronze grain size in cms., n_s the number of niobium filaments per unit area of cross-section of wire (number/cm^2), π has its usual meaning and r is the radius of the niobium filaments. Furthermore, defining f as the fractional area of cross-section which is Nb, we have,

$$n_s = \frac{f}{\pi r^2} \qquad (2).$$

In addition, the mean center to center Nb filament spacing (linear) in a cross-section is

$$\ell = \frac{1}{\sqrt{n_s}} \qquad (3)$$

so that the mean free bronze path distance between Nb filaments is $\ell - 2r$. Also, n_s is defined by N, the number of niobium filaments per cross-section

and d, the overall diameter of the wire in cms. such that $n_s \simeq \frac{4N}{\pi d^2}$. Table I shows calculations for these various limiting bronze grain size parameters for n_s and f values which are relative to the niobium/bronze superconducting multifilamentary wire geometry in the original hexagonal stacked regions of Nb rods. This table shows that the upper limit in the α bronze grain size is always larger than the mean free bronze path distance between Nb filaments, where the mean free bronze path is defined by $d/\sqrt{N}$. There are, however, several cases where (L/R) approaches 1 and this investigator believes these conditions correspond to many of the real cases in these Nb/bronze multifilamentary wires. Also, it should be pointed out that this analysis really sets an upper limit on the bronze grain size in the longitudinal direction of the wire.

Fig. 12 shows a photomicrograph of the etched grain structure of the IGC 0.0274 in. annealed multifilamentary wire in longitudinal section. It is clear from this figure that the mean free bronze path between the filaments is controlling the bronze grain size. Figs. 13, 14 and 15 are SEM photographs of the etched cross-sections of this IGC 0.0274 in.dia. wire. Fig. 13 clearly shows that the recrystallized grain size at the surface is quite large and that the grain size and sub-grain size of the bronze between the Nb filaments is quite fine. Figs. 14 and 15 show how really fine the grain size and sub-grain size microstructure is between the filaments. Figs. 16, 17 and 18 are SEM photographs of the same polished and etched IGC 0.0274 in.dia. wire shown in longitudinal section. Fig. 16 shows the annealed surface bronze grain size to be coarse and the microstructure between the filaments to be fine. Figs. 17 and 18 clearly show that extremely fine grain structure and microstructure between the Nb filaments in this wire. This type of observation was similar for the IGC 0.014 in. dia. and 0.017 in. dia. wires also (see footnote of Table I).

A Vickers hardness number profile was made on this wire moving from the outside edge where the coarse grain bronze exists to the center of

the wire. The VHN numbers were 100, 142, 186. 174, 212, and 218 as one moved progressively from the edge of the wire to its center. There is very little doubt, the fine grain structure and sub-grain structure of the bronze between the Nb filaments results in a marked increase in hardness and hence ultimate tensile strength of the material as one moves from the edge to the center of the wire cross-section.

Detailed studies of photographs similar to that of Figs. 12 through 18 for the IGC 0.0274 in. dia. wire revealed an f value of 0.377 and an L/R value of 0.613. A similar analysis for the 0.0114 in. dia. wire produced an f value of 0.54 and an L/R value 0.76. For the 0.017 in. IGC annealed wire, an f value of 0.53 and an L/R value of 0.73 were obtained. These values are clearly very close to the predicted values shown in Table 1, where the correlation of close agreement has been noted to the three wires as a footnote.

This study has revealed that the simple concept of slowing down migrating α bronze grain boundaries during recrystallization by second phase particles such as Nb filaments is far too simplistic with respect to what is actually occurring here. This concept places an upper limit on the α bronze grain size but in effect or actual practice the observed grain size or sub-grain size is considerably smaller than these predicted values.

Since large grains can form in the outer surface layer (see Fig. 13), the current investigator concludes any bronze high angle grain boundaries are dominantly lost at the Nb/bronze interfaces. The α bronze microstructure between the Nb filaments is essentially all sub-grain structure. This means the flow stress of the bronze rises rapidly as one draws the wire down. With increasing strain of the wire (i.e. reduction in cross-section), n_s goes up, R goes down and f remains constant.

This suggests the rise in the α bronze flow stress is going to be most severe the larger the accumulated drawing strain of the wire and the ability of inter-anneals to soften the bronze is less efficient.

Subsequent longitudinal draw stresses are going to rise and force the hard bronze to yield with attendant excessive distortion of the soft Nb filaments. The Nb filaments will become more distorted because they are now loaded in excess of their yield strength through longitudinal and tangential shear stresses. Figs. 19 and 20 are scanning electron micrograph cross-sections of the IGC 0.006 in. dia. annealed wire. The extensive Nb filament distortion is clearly evident. The Nb filament morphology in Fig. 20 should be compared to that of the IGC 0.0274 in. wire in Fig. 14.

In summary, the limiting bronze grain size effect as controlled by the Nb filaments in the manufacture of multi-filamentary Nb_3Sn superconducting wires appears to put an upper limit on the attainable bronze grain size. In actual practice the bronze grain size is less than this upper limit and is most frequently a sub-grain structure between filaments. This causes the flow stress of the bronze to rise with increased reductions in cross-sectional area of the wire and attendant loss in ductility results. The decreased fracture thoughness of the bronze at this later stage of the manufacturing process would allow fractures associated with discontinuous Nb filaments to propagate in an almost brittle manner. This could be one explanation for the increased incidence of wire draw breakages as one proceeds to finer and finer multifilamentary wires.

II(C) Bronze Ageing Studies and Attendant Attempts to Discern α Bronze Decomposition

II(c)(a) Hardness versus Ageing Time Studies

The hot/cold worked swaged 13 wt % Sn bronze rods prepared at Wright-Patterson Air Force Base in the Aero Propulsion Laboratory by 2nd Lt. Scott Holmes was used as the starting material to study ageing effects in this bronze alloy[4]. The rod material had a diameter of about 0.10 in. Fig. 21 shows a plot of the Vickers Hardness Number (VHN) versus ageing temperature for three different prior thermal/mechanical treatments of the bronze.

In Fig. 21, the data points depicted as strained, solution heat treated, quenched and aged all had the follwing treatment (designated ▽). The samples were compressed 65% and then solution heat treated at 520°C for 26 hours under a controlled Argon atmosphere and quenched into an ice water bath. The samples were aged extensive times at room temperature or at elevated temperatures for 25 hours in an Argon atmosphere and quenched again to room temperature. Each data point in this figure represents the average of at least 20 microhardness readings and this applies to all of the data for different thermal mechanical heat treatments.

The data points in this figure for the pretreatment solution heat treated, quenched and aged (designated □) means the specimens were heated to 520°C for 26 hours under an Argon atmosphere and quenched into ice water. The samples were then aged extensively at room temperature for 26 hours at the elevated ageing temperatures under the Argon atmosphere and quenched again to room temperature.

Finally, the data points depicted as solution heat treated, quenched, strained and aged (designated ○) means the samples were heated to 520°C for 26 hours and quenched into an ice water bath, and then compressively strained 65%. The samples were then allowed to age extensively at

room temperature for 25 hours at each respective ageing temperature under Argon. They were subsequently quenched into the ice water bath.

The Cu-Sn equilibrium phase diagram (see ref. 11) suggests that for a 13 wt % Sn bronze alloy, the α phase should decompose in the temperature range 350 to 425°C to α + δ, where the δ phase has a 31.83 wt % Sn composition. The δ phase should decompose into the α and ε phases at temperatures below 380 to 325°C. However, this transformation is extremely slow and for most purposes, δ can be considered as stable below 350°C.

The solubility of Sn in the α phase as depicted as decreasing significantly with decreasing temperature below 400°C appears to be only effective upon long annealing treatments after severe cold work. It was for these reasons that the present investigator decided to use the three different thermal/mechanical pretreatments employed to obtain the data of Figure 21.

There are several significant features to the data shown in Figure 21. Ageing up to 275°C of the quenched metastable γ phase for all three prior mechanical/thermal pretreatments shows a mild drop in the hardness or a slightly enhanced dultility, which is probably a stress relieving effect. The dramatic drop in hardness for the solution heat treated, quenched, strained and aged samples in the ageing temperature range 300 to 375°C could be due to the marked reduction in the dislocation density within the grains with very little attendant change in the α bronze grain size.

There does exist, however, a second possible explanation to this data. The problem lies in the samples which were solution heat treated, quenched, strained and aged, particularly with respect to the room temperature data point. The room temperature aged samples were set in "Koldmount self-curing resin" and the metallographic mount set up in

about 25 minutes at room temperature. Five days elapsed at room temperature (i.e. 120 hours) before the room temperature ageing data shown in Fig. 21 was obtained. At the time this data was being taken, the current investigator did not have a copy of Royet's report[1] and was unaware significant room temperature embrittlement after cold work might occur in period varying anywhere from 77 hours to 7 days at room temperature. It is therefore possible, that some hardening may have occurred in the solution heat treated, quenched, strained and aged samples at room temperature between essentially 0 hours and 120 hours. If this occurred then our results would somewhat substantiate Royet's observations, but this point remains unverified. This is one point which remains to be clarified since if some degree of hardening does occur within 120 hours at room temperature after extensive cold work, then it is most likely associated with very short range diffusion of Sn atoms to grain boundaries and dislocations. Consequently, a portion of the dramatic fall in hardness in the temperature range 300 to 350°C (see Fig. 21) could be associated with the "boiling-off" of the Sn atmospheres from grain boundaries and dislocations.

The present investigator considers a consistent change in microhardness of 10 VHN points as definitely suggestive of some sort of a hardening or embrittling reaction occurring in the metastable α bronze. Hence, the hardening observed for the two sets of samples, designated ∇ and $\square$ in Fig. 21. in the temperature range (300-400)°C as CD is considered significant. The metastable α could be decomposing into some coherent precipitate on its way to forming the ε phase. This interpretation is at least consistent with the age hardening observations of Chin et al[12] and Tisone et al[13] in rolled phosphor bronze prestrained 97%. The fact that the solution heat treated, quenched, strained and aged samples

(designated Fig. 21) exhibit an enhanced hardness of AB in Fig. 21 suggests the excessive prestrain has indeed probably formed some coherent precipitate on the way to forming δ above 350°C.

To further substantiate these observations a second set of samples were studied. These samples were cylindrical plugs of the 13 wt % Sn bronze cold press fit into rectangular brass blocks about 3 cm. long x 1-1/2 cm. wide by 0.5 cm. thick. Each brass block contained six 0.10 inch dia. bronze plugs. The brass blocks encapsulated in a quartz tube with an Argon atmosphere were solution heat treated at 465°C for 4 hours and quenched in an ice water bath. Each block was then aged for various times and various temperatures under an Argon atmosphere, and the hardness was measured. The resulting data of hardness versus ageing temperature is shown in Fig. 22. Beside each data point is shown the time in hours that the specimens were aged at each respective temperature except for 3 sets of samples which aged for months at room temperature prior to elevated temperature ageing tests. Each data point in this figure represents the average of at least 30 hardness readings which were always made at or near the center of the bronze plugs.

The data of Fig. 22, clearly shows absolutely no sign of any significant age hardening for extensive ageing times up to 200°C and in fact, the quench stress relieving effect is actually seen to be consistent with the data of Fig. 21. Again, we see definite signs of some age hardening of the order of 10 to 20 points VHN with ageing at 350 to 400°C for extensive times. The data of Fig. 22 is completely self-consistent with the data of Fig. 21. It should be pointed out that the thermal expansion coefficient of the bronze is less than that for the brass, so that the ageing of the bronze at elevated temperatures i.e. 350 and 400°C is not under a restrictive stress state.

At this point, the correlation of our ageing studies to the wire failure problems described by Royet[1] is not clear. We have not found evidence of an age embrittlement phenomena in this bronze in either the cold worked or solution treated material with ageing times in excess of months at either room temperature or 200°C. This statement is accurate only to the effect that we do not know if 65% compression strain of solution heat treated samples exhibits an age hardening effect at room temperature within 5 days or 120 hours. Royet[1] suggests the ageing problem is most likely associated with a sub optical microscopic embrittlement phenomena. The rather limited nature of Royet's[1] tests could support an alternative explanation such as we presented in the Introduction section, i.e these embrittling effects may be associated with cavity defects or Sn rich non-homogenized precipitates. However, the fact that the present data does suggest some form of strain induced transformatin in the 350 to 400°C range, prompted the current investigator to want to do transmission electron microscopy studies of a wide variety of samples in varied thermal/mechanical pretreatment states.

II(C)(b) Metallographic Studies

All of the samples tested and for which data is shown in Figs. 21 and 22 were polished and etched to reveal the microstructure and attempts to discern any second phase precipitation via optical metallography. The etching solutions for copper and its alloys employed in this study were from Smithells, Metalls Reference Book[8] , pages 326 and 327. In particular, solutions No. 2, No. 6 (6ml HCl, 19 gms Ferric chloride in 100 ml. of water) No. 6d (25 ml HCl, 8 gms Ferric chloride in 100 ml. of water) and No. 9 were employed. Etchant 9 was frequently followed with etching reagent 6. In addition to these three

etchants, experimentation with Livingston's[14] etchants to reveal dislocations on the {111} and {110} surfaces of copper was carried out on the Cu 13 wt % Sn bronze samples. Fig. 23 shows the microstructure of the 13 wt % Sn bronze samples solution heat treated, strained and aged at 299°C (see Fig. 21) after etching for 2 secs. in Reagent 9 followed by 2 secs in Reagent 6d. Fig. 24 shows the microstructure of the 13 wt % Sn bronze sample solely solution heat treated and aged at 299°C (see Fig. 21) after etching for 2 secs in Reagent 9 followed by 2 secs. in Reagent 6d. Comparison of Figs. 23 and 24 suggests the only difference one can discern between these two optical metallographic microstructures is that the much harder sample (Fig. 23 and Fig. 21) exhibits more sub-structure within the grains than the softer sample (Fig. 24 and Fig. 21).

Fig. 25 shows the typical microstructure as revealed by Livingston's[14] {111} face etchant for 15 secs. on the sample aged at 400°C for 77 hours in Fig. 22. Fig. 26 shows the typical microstructure as revealed by Livingston's[14] {111} face etchant for 30 secs. for the same samples as Fig. 25, only aged solely at room temperature. The rather marked differences in these etched microstructures within the α bronze grain boundaries was slightly suggestive of something significant may be going on with respect to α phase decomposition with 400°C ageing.

Fig. 27 is a photomicrograph at 2180 Mag. of the samples aged for 78 hours at 350°C (see Fig. 22) after etching in Reagent No. 2 for 5 secs. It certainly appeared we had indications of a grain boundary precipitate. Fig. 28 is a photomicrograph at 2180 Mag. of the same sample as for Fig. 27, yet this sample had been etched for 10 secs. in Livingston's {111} surface etchant. Again indications of some possible type of precipitation appeared.

At this point standard samples of Cu and Sn were made and mounted to fit into the Cambridge S4 Scanning Electron Microscope at the Manned Space Craft Center, Houston, Texas. The samples shown in Figs. 25 through 28 were studied by wave length dispersion analysis and dot profiles for Cu and Sn segregation. Absolutely no Sn segregation could be detected which means any form of real precipitaion must be well below several microns in dispersion wave-length. It became obvious, this study must use transmission electron micrographic techniques to look for any grain boundary or lattice coherent or incoherent type of precipitation phenomena.

II(C)(c) Planned Transmission Electron Microscope Studies

At this point the research started to run into serious problems. Firstly, the Philips EM200 (100 KV maximum)electron microscope in our laboratory had lens stabilizer problems and the high tension worked only satisfactorily to 60 KV. For these reasons a 3 month no new fund extension was requested for the grant which was approved. The electron microscope was finally fixed satisfactorily to do bright field transmission work about the 2nd week of December, 1982. Between Septebmer, 1982 and December 15, 1982, efforts were made to make up samples for study in the electron microscope.

Preparing samples for electron microscopic examination is always tedious and even more difficult when no one in the laboratory has had any prior experience with this 13 wt % Sn bronze alloy. The 0.10 in. dia. cylindrical 13 wt % Sn bronze rods were rolled down to sheet of thickness of about 90 microns. Three mm. discs were then punched out of the sheet. Samples were then heat treated under an Argon atmosphere to

reproduce many of the thermal/mechanical pretreatment described in Fig. 21. Another group of samples which had all of the thermal/mechanical pretreatments described in Fig. 21 were rolled down to discs of thicknesses varying from 60 to 170 microns.

All samples were then electrolytically thinned by the electro-polishing method until a hole is formed in the central region in a Struers Tenupol polishing tank unit with a Struers Polipower rectifier unit. The electrolyte used is that of 250 cc phosphoric acid, 250 cc ethyl alchol and 500 cc of distilled water at 12 volts at ambient temperature[15]. Some 50 samples have been prepared but numerous of them contain polishing defects. We have tried to fix up some of specimens by treatment in HNO_3 followed by water and alcohol rinses. We are optimistic some of the specimens will enable us to make transmission electron microscopic (TEM) examinations of the structure. This investigator may well have to experiment with other polishing solutions of the nitric acid/methonal type at 8-12 volts at low temperatures i.e. -20 to -60°C[13,16,17] in order to get good TEM samples free of polishing defects. It is further pointed out that our microscope is now operational at 100KV for bright field and electron-diffraction work, but the dark field set-up still needs some repair.

The current investigator planned to study the TEM samples which were prepared by December, 1982, during the Xmas break, i.e., the last 2 weeks of December. However, during this period, the main transformer which is housed in the steam tunnels servicing the Space Physics Bldg. was flooded out and burned out and our entire building was without power the entire end of the year break time from classes. At this time, it was too late to request a second no-new fund extension to this contract, so the effort to get some TEM studies accomplished failed.

II(C)(d) Contemplated Plans to Finish the Work

The current investigator intends to follow the room temperature ageing of this annealed 13 wt % Sn bronze, after 65% compressive deformation in the time period 30 minutes to 200 hours via microhardness studies. These results will either support or question the possible ageing effects described by Royet[1]. These results will also further substantiate the current investigators' interpretation of the data shown in Fig. 21 of this report.

The current investigator intends to continue to study the TEM thinned samples prepared under this contract for evidence of any α bronze decomposition products over a wide variation of prior thermal/mechanical histories.

II(D) Summary Comments

Once the above two works are complete, or most certianly after the room temperature ageing results are in, the current investigator feels he will probably have enough to say to possibly publish a paper. Such a paper may appear at an International Cryogenics Materials Conference and whose proceedings appear in "Advances in Cryogenic Engineering Materials" Plenum Press. The authors would be J.M. Roberts, W. Lindsay and A. Pendelton and any others who help with completing this study, particularly the TEM work.

From the standpoint of the manufacture of multifilamentary Nb_3Sn wires by the internal bronze process, a more extensive range of variables than this investigator has just described really needs to be investigated. The room temperature ageing of 13 wt % Sn bronze really needs to be followed over periods of 0 to 200 hours for varying initial bronze grain sizes (in the range 1 to 50 microns) and varied prestrains in the range 10% to 65%. Such a study should only be undertaken if the current investigator's contemplated plan to look for ageing in the coarse

grained bronze at 65% prestrain at room temperature yields results which support the possible ageing effect observations of Royet[1].

Mr. Wayne Lindsay and Mrs. Alice Pendleton, both of whom are Professional Masters Degree Candidates at Rice University have been associated with this research effort. These are non-thesis advanced degree candidates and this work collaboration was not part of the requirements for their anticipated degree. Mr. Lindsay's efforts formed part of his advanced metallurgical laboratory requirements for the B.Sc. degree and Mrs. Pendleton worked on the project in the summer.

The current investigator has not presented any of this work at a formal conference, meeting or seminar on or off campus at Rice University.

There has been no consultative and/or advisory functions to any other laboratories and agencies involved with this work, aside from the excellent interaction Dr. Roberts has had with Dr. Charles Oberly and co-workers at the Aero Propulsion Laboratory, Wright-Patterson Air Force Base, Ohio, 45433, since May of 1981. Dr. Roberts did use the SEM facilities at NASA Manned Space Craft Center to a limited extent in April of 1982.

The principal investigator does not claim any new discoveries, inventions or Patent Disclosure and Specific Applications stemming from the Research Effort.

The principal investigator still maintains an interest to bring this research effort to a conclusion which can lead to a publication. A period of time up to about two years may elapse before this investigator feels he has clarified the issues adequately to be worthy of publication. The current investigator would certianly be interested in any comments made by others who work in the field with respect to the ideas presented in this scientific report.

REFERENCES

(1) Jean M. Royet, "Ultrafine Filament Superconducting Niobium-Tin Braid," IGC's Final Report for Period August 1979 to September 1981 to Aero Propulsion Laboratory, WPAFB, Ohio, 45433, AFWAL-TR-82-2034 dated May 1982.

(2) J.C. Ho, C.E. Oberly, H.J. Garrett, M.S. Walker, B.A. Zeitlin and J.W. Ekin, Advances in Cryogenic Engineering Materials, vol. 27, pp.358-366, 1980.

(3) D.S. Holmes, A.M.Adair, C.E. Oberly, and J.C. Ho, "Bronze For Superconducting Wires" : The Powder Metallurgy Approach," IEEE Trans. Magn. Mag. Vol. 17, (1), pp. 1-3, 1980.

(4) John Melville Roberts, "A Metallurgical Investigation of the Internal Bronze Manufacturing Process of Nb_3Sn Superconducting Wire", 1981 USAF-SCEEE Faculty Research Program, Final Report, Submitted to Dr. Charles Oberly, WPAFB, Aero Propulsion Laboratory, September 15, 1981.

(5) A. H. Cottrell, Mechanical Properties of Matter, John Wiley and Sons, pg. 291, 1964.

(6) W.D. Kingery, H.K. Bowen, and D. R. Uhlmann, Introduction to Ceramics, John Wiley and Sons, pp. 197-200, 1960.

(7) American Society for Metals Handbook Committee, Metals Handbook 9th Edition, Vol. 2, *Properties and Selection: Nonferrous Alloys and Pure Metals*, ASM, Metals Park, Ohio, pp. 416 and 778, 1979.

(8) C. J. Smithells, ed., Metals Reference Book, 5th Edition (Butterworth, London) pp. 953-954, 1976.

(9) S. Okuda, M. Suenaga and T.S. Luhman, "Superconducting Current Densities in Bronze-Processed Nb_3Sn Multifilamentary Wires" Advances in Cryogenic Engineering Materials, Vol. 28, pp. 425-433, 1982.

(10) Robert E. Reed-Hill, Physical Metallurgy Principles, 2nd Editon, D. Van Nostrand pp. 316-318, 1973.

(11) M. Hansen, Constitution of Binary Alloys, Second Edition, McGraw-Hill, New York, pp. 633-637, 1985.

(12) G.Y. Chin, R.R. Hart, and B.C. Wonsiewicz, "Textured Phosphor Bronze-A Superior Spring Material," Trans. A.I.M.E., Vol. 245B, pp. 1669-1671, 1969.

(13) T. G. Tisone, G.Y. Chin and B. C. Wonsiewicz,"Precipitation in Rolled Phosphor Bronze", Metall. Trans. Vol. 1, pp. 2010-2011, 1970.

(14) J.D. Livingston, Acta Met. Vol. 10, pp. 229-239, 1962.

(15) I.S. Brammar and M.P.A. Dewey, Specimen Preparation for Electron Microscopy, Blackwell Scientific Publications, p.66, 1966.

(16) R.K. Ham and D. Jaffray, "Dislocation Multiplication, Vacancy Accumulation and the Onset of Jerky Flow During Forward and Reversed Strain in Cu-3.2At% Sn," Phil. Mag. Vol. 15, p. 247, 1967.

(17) M. De Bondt and A. Deruythere, "An α Phase in the Cu-16.5 At % Sn Alloy," Metall. Trans., Vol. 6A, pp. 537-544, 1975.

LIST OF FIGURES *

Figs. (1) through (11) (SEM) show typical examples of hair-line fractures associated with discontinuous Nb filaments in 0.0274 in. dia. IGC Nb/bronze polished wire in longitudinal section.

Figs. 1, 2, 3, 6, 9, 10 and 11 are at 1000 Mag.

Figs. 4, 5, 7, and 8 are at 350 X.

Fig (12) shows the grain structure of the bronze between Nb filaments in 0.0274 in IGC Nb/bronze wire in longitudinal section. Mag. 800X.

Figs. (13), (14) and (15) (SEM) show the surface grain structure and the inter Nb filament bronze grain and sub-grain structure in 0.0274 in. dia. IGC Nb/bronze wire in cross-section. Figs. (13) and (14) are at 1000 X.

Fig. 15 is at 200 X.

Figs. (16, (17), and (18) (SEM) show the surface and the inter Nb filament bronze grain and sub-grain structure in 0.0274 in. dia. IGC Nb/bronze wire in longitudinal section. Figs. (16) and (17) are at 1000 X.

Fig. (18) is at 3000 X.

Figs. (19) and (20) (SEM) show the extensive geometrical distortion of the Nb filaments in cross-section in IGC Nb/bronze wire of 0.006 in. dia.

Fig. (19) is at 5000 X. Fig. (20) is at 10,000 X.

*The negatives of these Figures are retained by Dr. Roberts at Rice University. White glossy prints will be provided to very interested persons upon specific request. All photographs reduced 40% in reproduction.

Fig. (21) Vickers Hardness Number versus Ageing Temperature for 13 wt. % Sn bronze samples.

○ - solution heat treated-quenched-strained-aged.

▽ - strained - solution heat treated - quenched -aged

□ - solution heat treated - quenched - aged.

Fig. (22) Vickers Hardness Number versus Ageing Temperature for 13 wt % Sn bronze plugs embedded in a brass matrix plate. Ageing times in hours shown for the various temperatures and samples beside each data point. Initial state means as solution heat treated and quenched.

Fig. (23) 13wt % Sn bronze microstructure at 1000X. Etched 2 secs in No. 9 and 2 secs. in No. 6d reagents. Thermal/mechanical pretreatment - solution heat treated, quenched -strained and aged at 299°C (See Fig. 21).

Fig. (24) 13 wt % Sn bronze microstructure at 1000X. Etched 2 secs. in No. 9 and 2 secs. in No. 6d reagents. Thermal/mechanical pretreatment - solution heat treated - quenched -aged at 299°C (See Fig. 21).

Fig. (25) 13 wt % Sn bronze plug microstructure at 2180 X. Thermal pretreatment - solution treated - quenched and aged at 400°C for 77 hours (see Fig. 22). Etched 15 secs in Livingston's[14] {111} etchant.

Fig. (26) 13 wt % Sn bronze plug microstructure at 2180 X. Thermal pretreatment- solution treated - quenched and aged at room temperature for months (see Fig. 22) Etched 30 secs. in Livingston's[14] {111} etchant.

Fig. (27) 13 wt % Sn bronze plug microstructure at 2180 X. Thermal pretreatment -solution heat treated - quenched - aged for 78 hours at 350°C (see Fig. 22). Etched for 5 secs. in Reagent No. 2. (see text)

Fig. (28) 13 wt % Sn bronze plug microstructure at 2180 X. Thermal pretreatment-solution heat treated - quenched - aged for 78 hours at 350°C (see Fig. 22). Etched for 10 secs. in Livingston's[14] {111} etchant.

TABLE I

LIMITING BRONZE GRAIN SIZE PARAMETERS

	(n) No. of Nb filaments per cross-section	(d) Overall diameter of wire cms.	(n_s) Number of Nb filaments per unit area of wire cross section (number/cm^2)	(r) Radius of the Nb filaments in cms.	(R) Upper limit on the α bronze grain size cms.	(ℓ) Mean center to center Nb filament Spacing (linear) in a cross-section in cms.	(ℓ-2r) Mean free bronze path distance between Nb filaments (cms.)	(L) Mean free path in bronze $= d/\sqrt{N}$ in cms.	(L)/(R) ratio	f
	1000	0.01524	5.4813×10^{6}	5×10^{-6}	2.32×10^{-2}	4.2713×10^{-4}	4.1713×10^{-4}	4.76×10^{-4}	0.021	0.00043
	1000	0.01524	5.4813×10^{6}	1×10^{-4}	1.20×10^{-3}	4.2173×10^{-4}	2.2713×10^{-4}	4.76×10^{-4}	0.397	0.17222
	1000	0.0254	1.9733×10^{6}	5×10^{-6}	6.45×10^{-2}	7.1187×10^{-4}	7.0187×10^{-4}	7.9×10^{-4}	0.012	0.00016
	1000	0.0254	1.9733×10^{6}	1×10^{-4}	3.20×10^{-3}	7.1187×10^{-4}	5.1187×10^{-4}	7.9×10^{-4}	0.247	0.0620
	10^4	0.01524	5.4813×10^{7}	5×10^{-6}	2.32×10^{-3}	1.3506×10^{-4}	1.2507×10^{-4}	1.524×10^{-4}	0.066	0.00430
	10^4	0.0254	1.9733×10^{7}	5×10^{-6}	6.45×10^{-4}	2.2511×10^{-4}	2.1511×10^{-4}	2.54×10^{-4}	0.394	0.00155
(1)	10^4	0.0254	1.9733×10^{7}	1×10^{-4}	3.20×10^{-4}	2.2511×10^{-4}	2.511×10^{-5}	2.54×10^{-4}	0.794	0.6200
	10^5	0.01524	5.4813×10^{8}	5×10^{-6}	2.32×10^{-4}	4.2713×10^{-5}	3.2713×10^{-5}	4.8×10^{-5}	0.207	0.04306
	10^5	0.0254	1.9733×10^{8}	5×10^{-6}	6.45×10^{-4}	7.1188×10^{-5}	6.1188×10^{-5}	8.03×10^{-5}	0.124	0.01550
(2)	1600	0.0254	3.157×10^{6}	2×10^{-4}	1×10^{-3}	5.628×10^{-4}	1.628×10^{-4}	6.35×10^{-4}	0.635	0.397
	1600	0.0254	3.157×10^{6}	1×10^{-4}	2×10^{-3}	5.6281×10^{-4}	3.6281×10^{-4}	6.35×10^{-4}	0.318	0.09919
	1600	0.01524	8.77×10^{6}	1×10^{-4}	7.26×10^{-4}	1.3768×10^{-4}	1.3768×10^{-4}	3.80×10^{-4}	0.523	0.27555
	1600	0.0508	7.893×10^{5}	1×10^{-5}	8.06×10^{-2}	1.1256×10^{-3}	1.1056×10^{-3}	1.27×10^{-3}	0.016	0.00025
	1600	0.0508	7.893×10^{5}	2×10^{-4}	4.03×10^{-3}	1.1256×10^{-3}	7.256×10^{-4}	1.27×10^{-3}	0.315	0.09920
	1600	0.203	4.943×10^{4}	4×10^{-5}	6.44×10^{-1}	4.4978×10^{-3}	4.4178×10^{-3}	5.075×10^{-3}	0.008	0.00025
	1600	0.203	4.943×10^{4}	8×10^{-4}	1.61×10^{-2}	4.4978×10^{-3}	2.8978×10^{-3}	5.075×10^{-3}	0.315	0.09940
(3)	1600	0.01524	8.77×10^{6}	1.5×10^{-4}	4.84×10^{-4}	1.3768×10^{-4}	3.768×10^{-5}	3.80×10^{-4}	0.83	0.62

(1) Conditions correspond closely to IGC's 0.0114 in. dia. wire.
(2) Conditions correspond closely to IGC's 0.0274 in. dia. wire.
(3) Conditions correspond closely to IGC's 0.017 in. dia. wire.

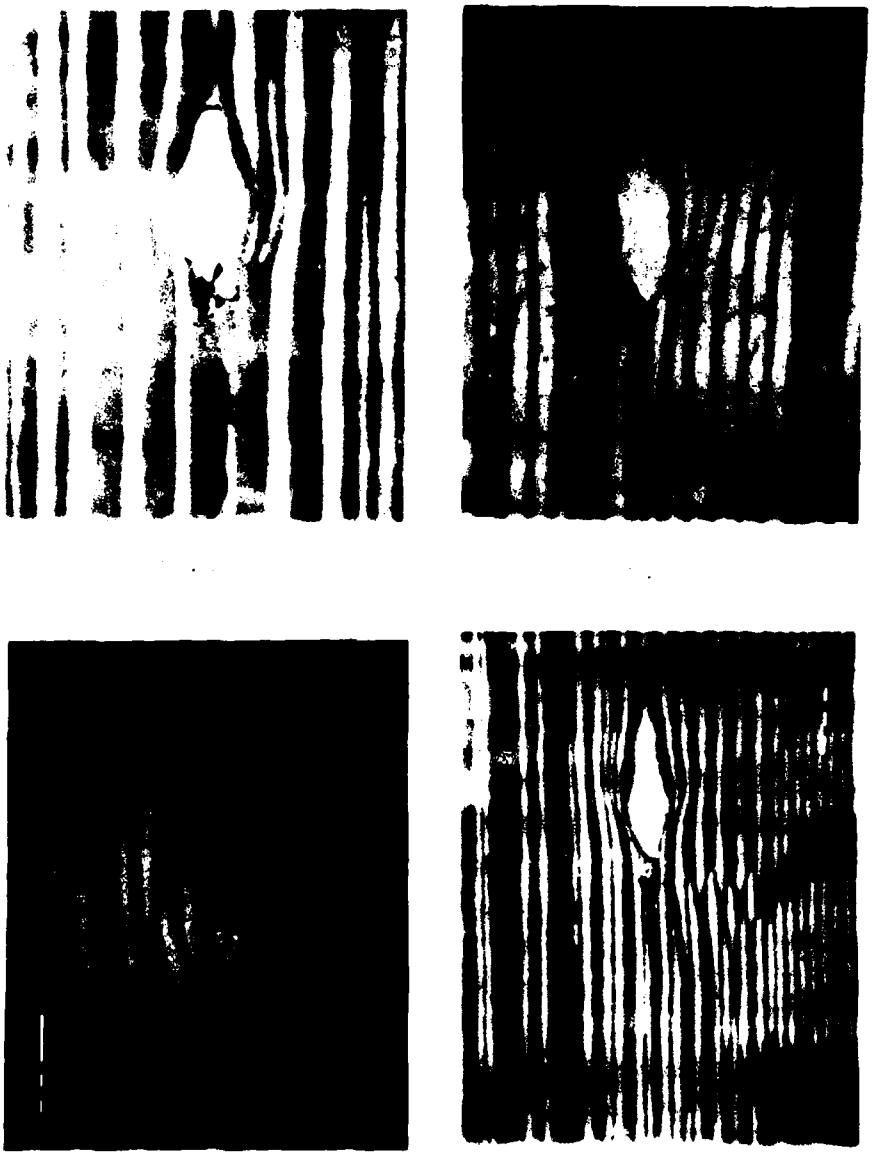

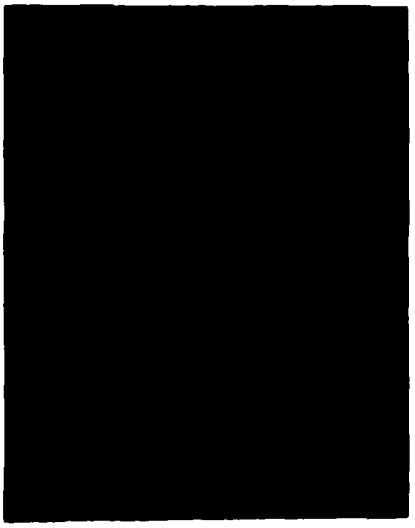

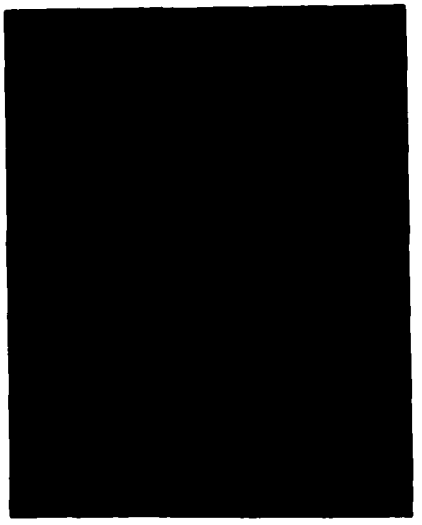

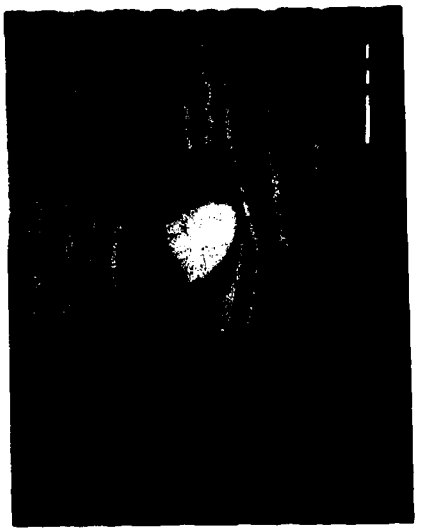

FIG. 9

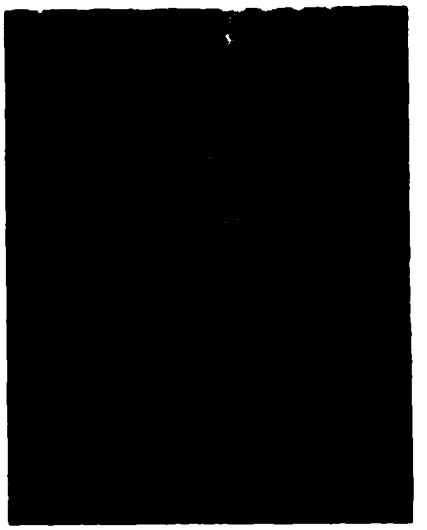

FIG. 10

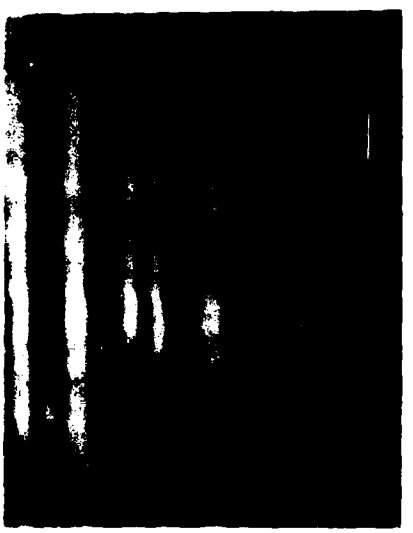

FIG. 11

FIG. 12

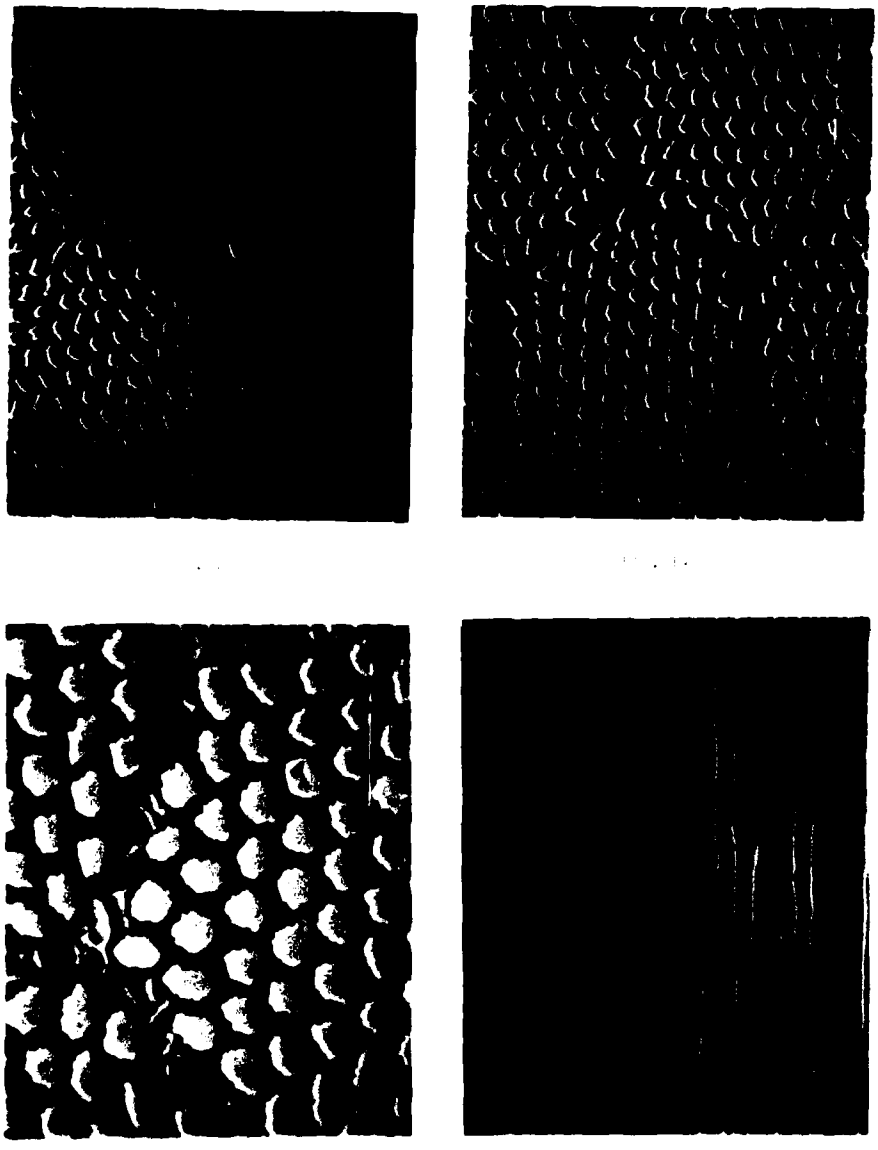

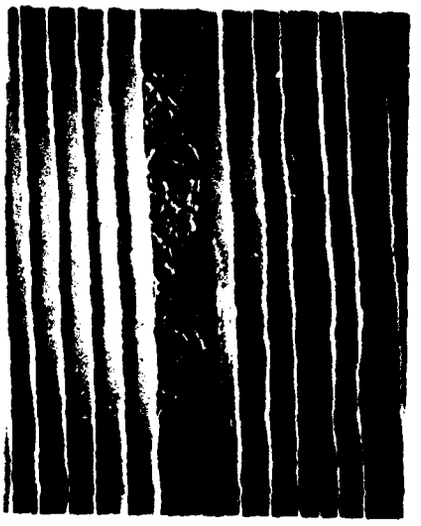

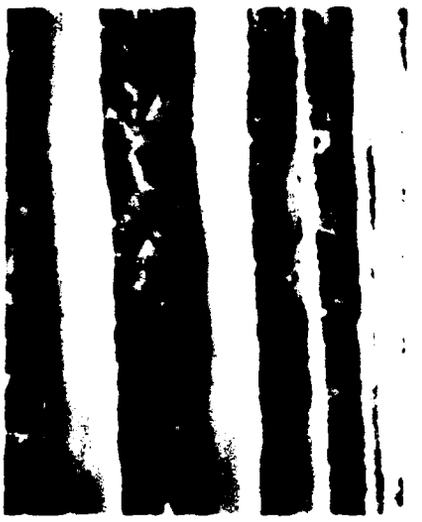

FIG. 18

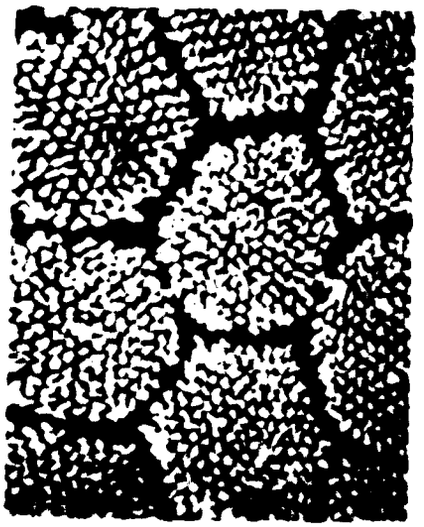

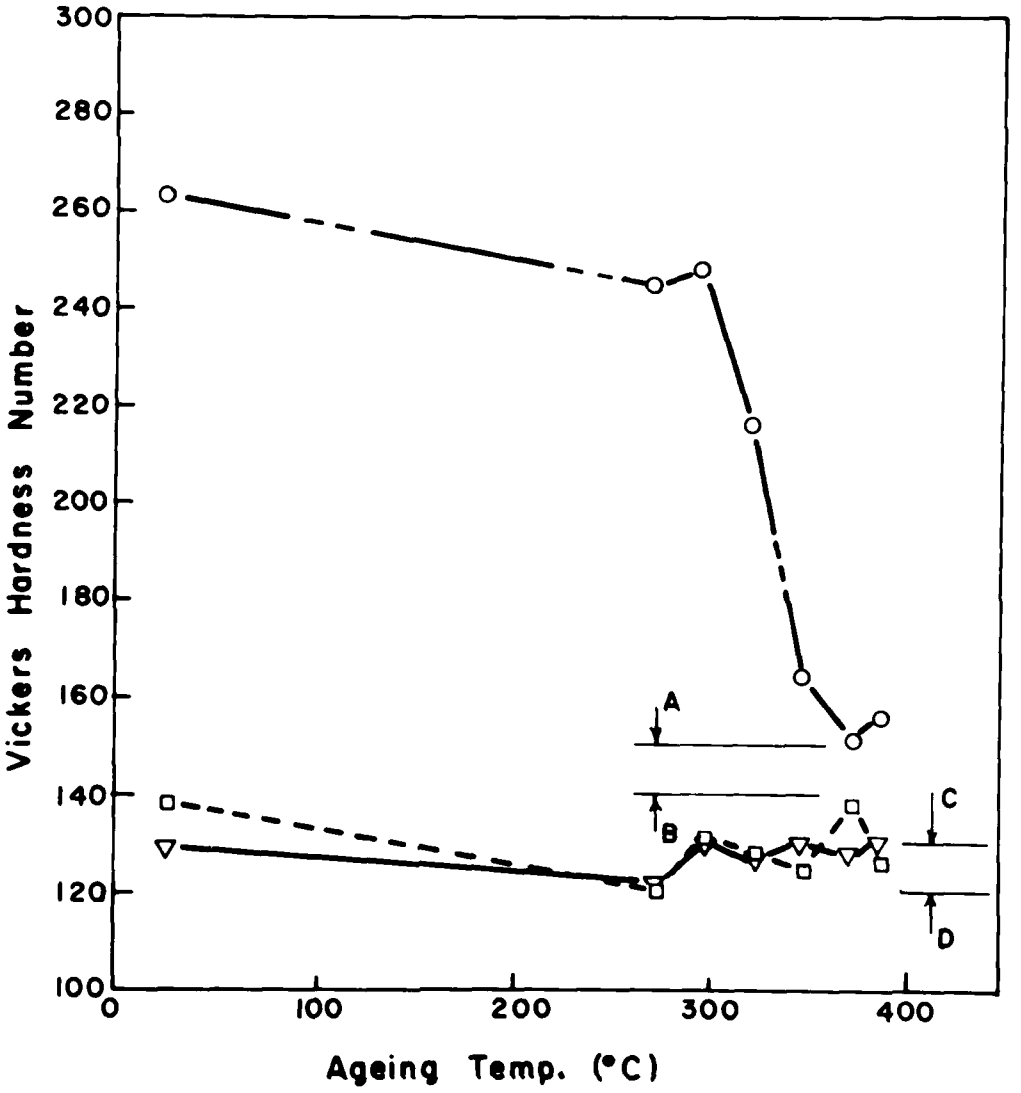
300
280
260
240
220
200
180
160
140
120
100
0
100
200
300
400
Vickers Hardness Number
Ageing Temp. (°C)
A
B
C
D

fig. 21

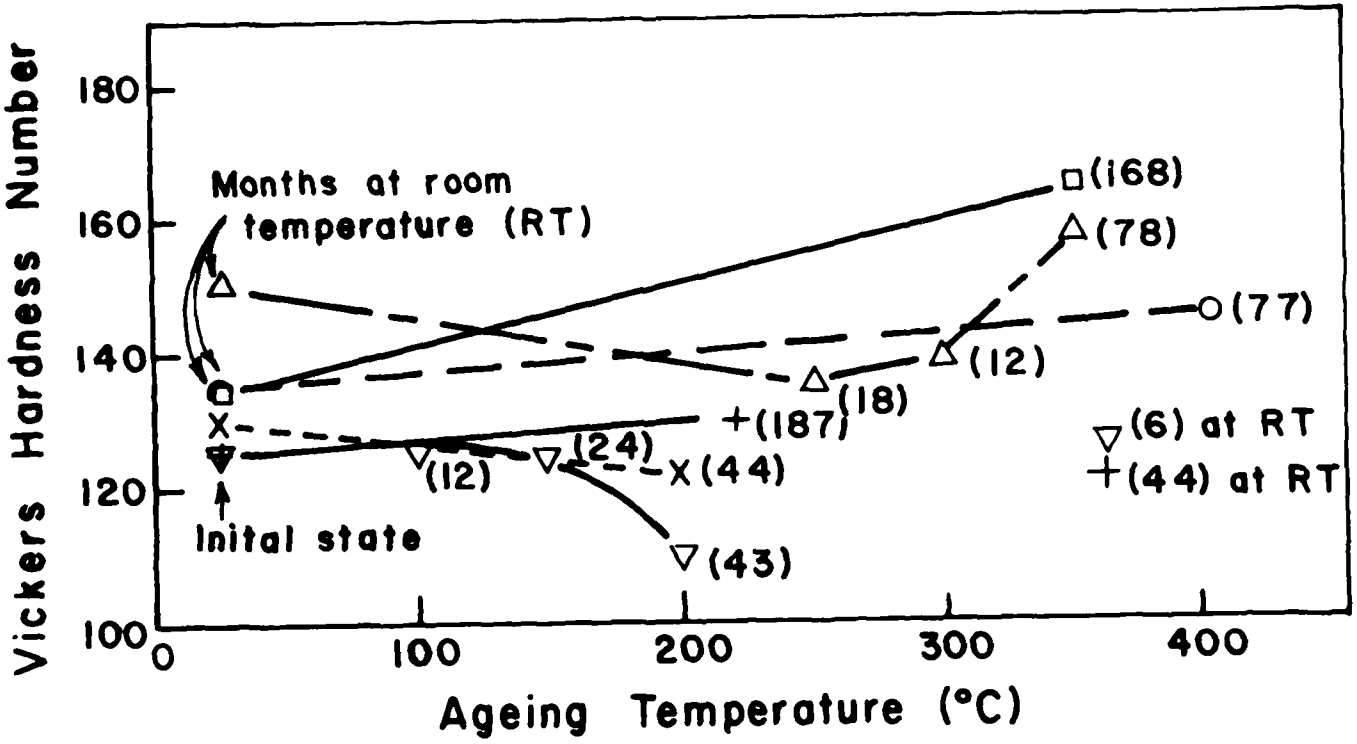
Vickers Hardness Number
180
160
140
120
100
0
100
200
300
400
Ageing Temperature (°C)
Months at room temperature (RT)
Inital state
(168)
(78)
(77)
(12)
(18)
(187)
(24)
(12)
(44)
(43)
(6) at RT
(44) at RT

fig. 22

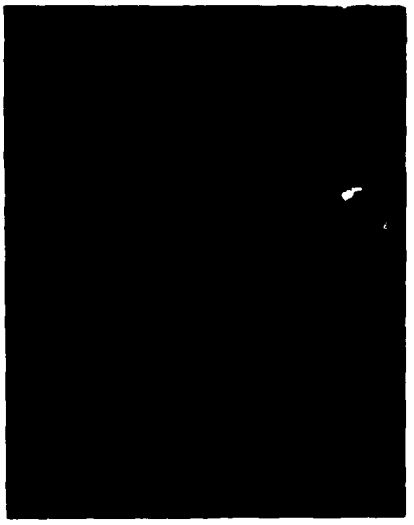

FIG. 23

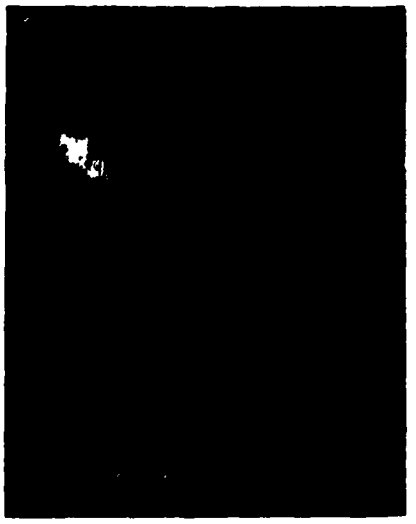

FIG. 24

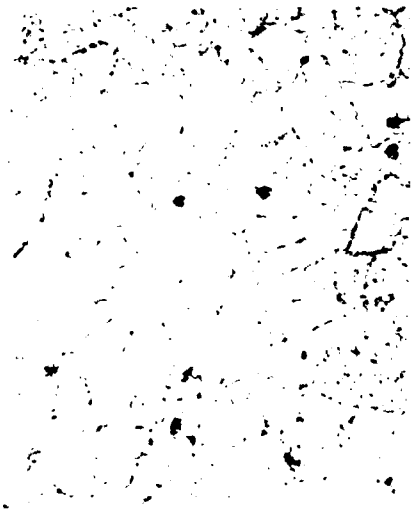

FIG. 25

FIG. 26

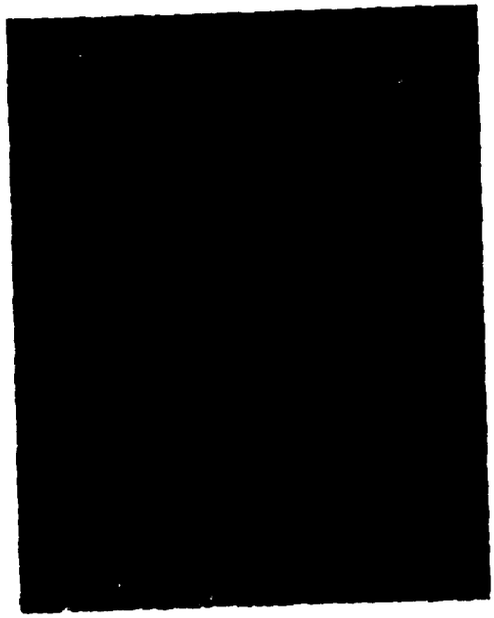

FIG. 37

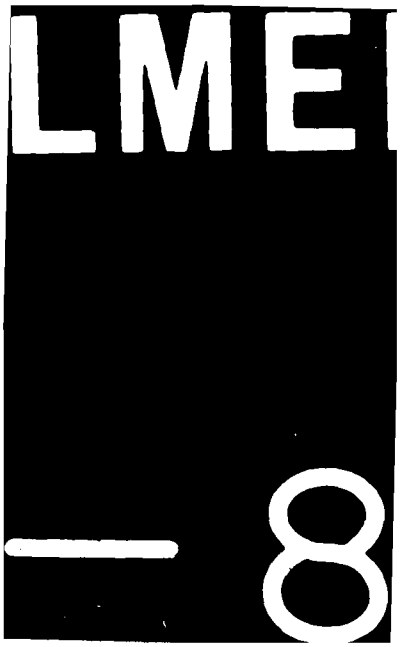
LME
8